7. E. B. Shera, N. K. Seitzinger, L. M. Davis, R. A. Keller, S. A. Soper, *Chem. Phys. Lett.* **174**, 553 (1990).
8. W. E. Moerner and L. Kador, *Anal. Chem.* **61**, A1217 (1989).
9. W. E. Moerner, and M. Orrit, *Science* **283**, 1670 (1999).
10. E. Betzig and R. J. Chichester, *ibid.* **262**, 1422 (1993).
11. J. K. Trautman, J. J. Macklin, L. E. Brus, E. Betzig, *Nature* **369**, 40 (1994).
12. X. S. Xie and R. C. Dunn, *Science* **265**, 361 (1994).
13. W. P. Ambrose, P. M. Goodwin, J. C. Martin, R. A. Keller, *Phys. Rev. Lett.* **72**, 160 (1994).
14. ———, *Science* **265**, 364 (1994).
15. R. X. Bian, R. C. Dunn, X. S. Xie, P. T. Leung, *Phys. Rev. Lett.* **75**, 4772 (1995).
16. J. J. Macklin, J. K. Trautman, T. D. Harris, L. E. Brus, *Science* **272**, 255 (1996).
17. J. K. Trautman and J. J. Macklin, *Chem. Phys.* **205**, 221 (1996).
18. T. Funatsu, Y. Harada, M. Tokunaga, K. Saito, T. Yanagida, *Nature* **374**, 555 (1995).
19. I. Sase, H. Miyata, J. E. T. Corrie, J. S. Craik, K. Kinosita, *Biophys. J.* **69**, 323 (1995).
20. R. D. Vale *et al.*, *Nature* **380**, 451 (1996).
21. T. Schmidt, G. J. Schutz, W. Baumgartner, H. J. Gruber, H. Schindler, *J. Phys. Chem.* **99**, 17662 (1995).
22. R. M. Dickson, D. J. Norris, Y. L. Tzeng, W. E. Moerner, Science **274**, 966 (1996).
23. J. H. Jett *et al.*, *J. Biomol. Struct. Dyn.* **7**, 301 (1989).
24. R. A. Keller *et al.*, *Appl. Spectrosc.* **50**, A12 (1996).
25. M. Eigen and R. Rigler, *Proc. Natl. Acad. Sci. U.S.A.* **91**, 5740 (1994).
26. U. Mets and R. Rigler, *J. Fluoresc.* **4**, 259 (1994).
27. S. M. Nie, D. T. Chiu, R. N. Zare, *Science* **266**, 1018 (1994).
28. J. Mertz, C. Xu, W. W. Webb, *Opt. Lett.* **20**, 2532 (1995).
29. L. Brand, C. Eggeling, C. Zander, K. H. Drexhage, C. A. M. Seidel, *J. Phys. Chem.* **101**, 4313 (1997).
30. E. J. Sanchez, L. Novotny, G. R. Holtom, X. Sunney Xie, *ibid.*, p. 7019.
31. S. C. Hill, H. I. Saleheen, M. D. Barnes, W. B. Whitten, J. M. Ramsey, *Appl. Opt.* **35**, 6278 (1996).
32. T. Basché, W. E. Moerner, M. Orrit, U. P. Wild, Eds., *Single-molecule Optical Detection, Imaging and Spectroscopy* (Wiley-VCH, Weinheim, Germany, 1997).
33. J. K. Trautman and W. P. Ambrose, in (*32*), pp. 191–222.
34. X. S. Xie, *Acc. Chem. Res.* **29**, 598 (1996).
35. ———, in *Focus on Multidimensional Microscopy*, P. C. Chen, P. P. Hwang, J. L. Wu, G. Wang, H. Kim, Eds. (World Scientific, Singapore, 1997), vol. 1.
36. S. M. Nie and R. N. Zare, *Annu. Rev. Biophys. Biomol. Struct.* **26**, 567 (1997).
37. X. S. Xie and J. K. Trautman, *Annu. Rev. Phys. Chem.* **49**, 441 (1998).
38. Q. Xue and E. S. Yeung, *Nature* **373**, 681 (1995).
39. D. B. Craig, E. A. Arriaga, J. C. Y. Wong, H. Lu, N. J. Dovichi, *J. Am. Chem. Soc.* **118**, 5245 (1996).
40. W. Tan and E. S. Yeung, *Anal. Chem.* **69**, 4242 (1997).
41. H. P. Lu, L. Xun, X. S. Xie, *Science* **282**, 1877 (1998).
42. A. H. Iwane *et al.*, *FEBS Lett.* **407**, 235 (1997).
43. D. W. Pierce, N. Hom-Booher, R. D. Vale, *Nature* **388**, 338 (1997).
44. L. Romberg, D. W. Pierce, R. D. Vale, *J. Cell Biol.* **140**, 1407 (1998).
45. A. Miyawaki *et al.*, *Nature* **388**, 882 (1997).
46. Y. Suzuki, T. Yasunaga, R. Ohkura, T. Wakabayashi, K. Sutoh, *ibid.* **396**, 380 (1998).
47. J. Llopis, J. McCaffery, A. Miyawaki, M. G. Farquhar, R. Y. Tsien, *Proc. Natl. Acad. Sci. U.S.A.* **95**, 6803 (1998).
48. S. J. Anthony-Cahill, M. C. Griffith, C. J. Noren, D. J. Suich, P. G. Schultz, *Trends Biochem. Sci.* **14**, 400 (1989).
49. V. W. Cornish *et al.*, *Proc. Natl. Acad. Sci. U.S.A.* **91**, 2910 (1994).
50. G. J. Schütz, H. Schindler, T. Schmidt, *Biophys. J.* **73**, 1073 (1997).
51. X- H. Xu and E. S. Yeung, *Science* **275**, 1106 (1997).
52. ———, *ibid.* **281**, 1650 (1998).
53. E. Betzig, *Opt. Lett.* **20**, 237 (1995).
54. T. Ha, T. Enderle, D. S. Chemla, S. Weiss, *IEEE J. Select. Top. Quantum Electronics* **2**, 1115 (1996).
55. A. M. van Oijen, J. Köhler, J. Schmidt, M. Müller, G. J. Brakenhoff, *Chem. Phys. Lett.* **292**, 183 (1998).
56. G. J. Schütz, W. Trabesinger, T. Schmidt, *Biophys. J.* **74**, 2223 (1998).
57. T. Förster, *Ann. Phys.* **2**, 55 (1948).
58. L. Stryer and R. P. Haugland, *Proc. Natl. Acad. Sci. U.S.A.* **58**, 719 (1967).
59. P. R. Selvin, *Methods. Enzymol.* **246**, 300 (1995).
60. T. Ha *et al.*, *Proc. Natl. Acad. Sci. U.S.A.* **93**, 6264 (1996).
61. T. Ha *et al.*, *ibid.* **96**, 893 (1999).
62. T. Ha *et al.*, in preparation.
63. A. A. Deniz, *Proc. Natl. Acad. Sci. U.S.A.*, in press.
64. M. Dahan *et al.*, in preparation.
65. T. Ha, T. Enderle, D. S. Chemla, P. R. Selvin, S. Weiss, *Phys. Rev. Lett.* **77**, 3979 (1996).
66. I. Sase, H. Miyata, S. Ishiwata, K. Kinosita, *Proc. Natl. Acad. Sci. U.S.A.* **94**, 5646 (1997).
67. D. M. Warshaw *et al.*, *ibid.* **95**, 8034 (1998).
68. S. C. Hopkins *et al.*, *Biophys. J.* **72**, A1 (1997).
69. T. Ha, J. Glass, T. Enderle, D. S. Chemla, S. Weiss, *Phys. Rev. Lett.* **80**, 2093 (1998).
70. W. P. Ambrose, P. M. Goodwin, J. P. Nolan, *Bioimaging*, in press.
71. M. Sauer *et al.*, *ibid.* **6**, 14 (1998).
72. C. Eggeling, J. R. Fries, L. Brand, R. Gunther, C. A. Seidel, *Proc. Natl. Acad. Sci. U.S.A.* **95**, 1556 (1998).
73. J. Glass, in preparation.
74. H. Wu, Z. Hu, X.-Q. Liu, *Proc. Natl. Acad. Sci. U.S.A.* **95**, 9226 (1998).
75. A. D. Mehta, M. Rief, J. A. Spudich, D. A. Smith, R. M. Simmons, *Science* **283**, 1689 (1999).
76. J. K. Gimzewski and C. Joachim, *ibid.*, p. 1683.
77. A. Ishijima *et al.*, *Cell* **92**, 161 (1998).
78. S. B. Smith, Y. Cui, C. Bustamante, *Science* **271**, 795 (1996).
79. T. R. Strick, J.-F. Allemand, D. Bensimon, A. Bensimon, V. Croquette, *ibid.*, p. 1835.
80. M. S. Kellermayer, S. B. Smith, H. L. Granzier, C. Bustamante, *ibid.* **276**, 1112 (1997).
81. M. Rief, M. Gautel, F. Oesterhelt, J. M. Fernandez, H. E. Gaub, *ibid.*, p. 1109.
82. L. Tskhovrebova, J. Trinick, J. A. Sleep, R. M. Simmons, *Nature* **387**, 308 (1997).
83. K. Svoboda, C. F. Schmidt, B. J. Schnapp, S. M. Block, *ibid.* **365**, 721 (1993).
84. L. M. Mannuzzu, M. M. Moronne, E. Y. Isacoff, *ibid.* **271**, 213 (1996).
85. M. J. Bruchez Jr., M. M. Moronne, P. Gin, S. Weiss, P. A. Alivisatos, *ibid.* **281**, 2013 (1998).
86. W. C. W. Chan and S. Nie, *ibid.*, p. 2016.
87. Two drug-discovery companies are already promoting fluorescence correlation spectroscopy (FCS) and single-molecule detection as a means for high-throughput screening (Evotec and Molecular Machines).

88. I am indebted to A. P. Alivisatos, U. Banin, M. Bruchez, D. S. Chemla, M. Dahan, A. A. Deniz, Th. Enderle, J. Glass, J. Grunwell, T. Ha, Th. Lacoste, T. Laurence, J. Liang, A. Martin, P. G. Schultz, P. R. Selvin, and A.Y. Ting for their contributions to the single-molecule spectroscopy effort in Berkeley, and to S. R. Bolton, M. Dahan, J. Glass, T. Ha, and Th. Lacoste for critical reading of the manuscript. This work was supported by the Laboratory Directed Research and Development Program of Lawrence Berkeley National Laboratory under the U.S. Department of Energy, contract DE-AC03-76SF00098 and Office of Naval Research Contract N0001498F0402.

REVIEW

Nanoscale Science of Single Molecules Using Local Probes

James K. Gimzewski[1]* and Christian Joachim[2]

Experiments on individual molecules using scanning probe microscopies have demonstrated an exciting diversity of physical, chemical, mechanical, and electronic phenomena. They have permitted deeper insight into the quantum electronics of molecular systems and have provided unique information on their conformational and mechanical properties. Concomitant developments in experimentation and theory have allowed a diverse range of molecules to be studied, varying in complexity from simple diatomics to biomolecular systems. At the level of an individual molecule, the interplays of mechanical and electronical behavior and chemical properties manifest themselves in an unusually clear manner. In revealing the crucial role of thermal, stochastic, and quantum-tunneling processes, they suggest that dynamics is inescapable and may play a decisive role in the evolution of nanotechnology.

In 1952, Erwin Schrödinger wrote that we would never experiment with just one electron, atom, or molecule (*1*). Eight years later, Richard P. Feynman told us that there are no physical limitations to arranging atoms the way we want (*2*). By the early 1980s, scanning tunneling microscopy (STM) (*3*) radically changed the ways we interacted with and even regarded single atoms and molecules. The very nature of proximal probe methods encourages exploration of the nanoworld beyond conventional microscopic imaging. Scanned probes now allow us to perform "engineering" operations on single molecules, atoms, and bonds, thereby providing a tool that operates at the ultimate limits of fabrication. They have also enabled exploration of molecular properties on an individual nonstatistical basis.

Molecules represent an amazingly diverse range of structures and associated properties. Their complexity increases through the fields

of organic chemistry to supramolecular chemistry, synthetic polymers, and finally biomolecular systems. This diversity has promulgated a wide variety of scanning probe microscopy (SPM) tools to investigate molecular properties. Furthermore, the dimensions of synthetic molecular systems now overlap with the levels of miniaturization in microelectronics and with the length scales of biological systems. This suggests that "bottom-up" approaches to nanofabrication may one day compete with conventional "top-down" approaches in providing nanotechnologies for the next millennium. "Top-down" refers to increased miniaturization through extension of existing microfabrication schemes. Conversely, the bottom-up scenario is one of ever-increasing complexity at the molecular level while maintaining control on an atom-by-atom basis.

The first attempts at imaging biological molecules using STM date back to 1983 (*4*). In 1987, individual molecules of phthalocyanine, lipid bilayers, and ascorbic acid were reported (*5*). Ohtani *et al.* imaged benzene, the molecule of Kekules' dream, as three-lobed rings in 1988 (*6*). Today, molecular imaging is a starting point for nanoscale experiments as well as being an everyday tool employed in many research disciplines.

Conformational Mechanics

Direct real-space imaging by STM. Molecular conformation is often subtle, and the degrees of freedom in complex molecules result in an enormous variety of molecular forms and properties. A number of approaches have been developed to investigate conformational and mechanical properties of single molecules by SPM, in which applicability depends on the flexibility and the complexity of the molecule under investigation. Semiflexible molecules have been studied by direct real-space imaging with STM. For example, Cu-tetra (3,5-di-*tert*-butyl phenyl) porphyrin (Cu-TDBPP) molecules have been shown to adapt conformationally to different metallic substrates by principal σ-bond rotations of the four di-*tert*-butyl phenyl (DTBP) groups symmetrically bound to the central porphyrin ring of the molecule (*7*). These four bulky groups determine the shape of the molecule, which is imaged by STM as four lobes, and also define the interaction of the molecule with the substrate. The patterns of the four lobes allowed determination of the dihedral rotation angles of the DTBP substituents, which range from 90° down to 30°, depending on the crystallography and the chemistry of the surface (Fig. 1, A through D). Similar STM recognition of conformational form has been demonstrated for the photochromic molecule bianthrone (*8*), and it was shown recently by STM that conformational mobility of discotic liquid crystals, containing flexible alkoxy side chains, is sufficient to induce chirality in nonchiral molecules (*9*).

Single-molecule force spectroscopy. Although the imaging approach works well for semirigid molecules, it is unsuited to systems with high degrees of conformational freedom, such as the long flexible molecules predominant in biology and polymer science. Such molecular chains can adapt their shape by noncovalent interactions acting on a wide variety of levels of organizational scales, resulting for example in helical, sheet-, and chainlike structures. Single-molecule force spectroscopy (SMFS) has allowed the mechanical properties of such molecules to be investigated with piconewton sensitivity and subnanometer accuracy. By moving a functionalized atomic force microscope (AFM) tip toward the surface with a whiplike action, single-molecular binding can be achieved because of the molecular dimensions of the tip apex. The response of the cantilever upon retraction provides not only the strengths of two binding interactions but also detailed insights into the energetics and mechanics of structural phase transitions, conformational changes, and the unfolding of stretched molecules. Accessible interactions include (i) rupture forces in the 50- to 300-pN range by breaking antigen-antibody or receptor-

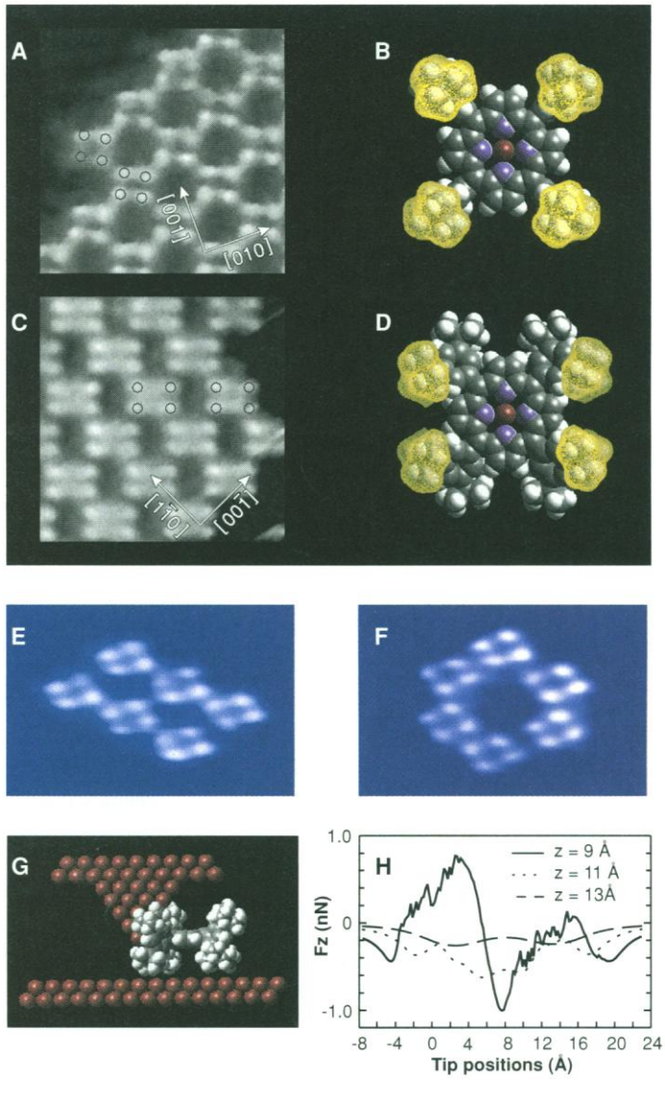

Fig. 1. (**A** through **D**) Conformational identification of Cu-DTBPP molecules at room temperature. The STM images of each molecule display a four-lobed pattern in a square arrangement when adsorbed on Cu(100) (A), which changes to a rectangular form on Ag(110) (C). The corresponding molecular models of Cu-DTBPP in (B) and (D) show the four DTBPP groups, highlighted in yellow, which are responsible for patterns seen in the STM images in (A) and (C). The bond rotations of the TBPP groups of 90° and 30° in (B) and (D), respectively, fit well with the STM images. (A) through (D) are reprinted with permission from *Nature* (*28*). Copyright 1997 Macmillan Magazines, Ltd. (*28*). (**E** through **H**) Room-temperature repositioning of molecules. (E) and (F) show STM images (26 nm by 26 nm in size) of six Cu-TBPP molecules before and after a sequence of lateral positioning steps using the STM tip. The final structure shows no evidence of molecular disruption and contains in total over 1000 atoms in a hexameric form that is unnatural for adsorption on the Cu(100) substrate. Elastic-scattering quantum chemistry calculations, coupled with molecular mechanics, were used to show that molecular conformational changes occurred during repositioning [side view shown in (G)]. The crossover from squeezing the molecule to lateral displacement depends on the tip altitude, z, shown in plots of the force (Fz) versus tip position in (H). Lateral motion occurs by a slip-stick mechanism. (E) and (H) are from (*7*).

[1]IBM Research Division, Zurich Research Laboratory, 8803 Rüschlikon, Switzerland. [2]Centre d'Elaboration des Matériaux et d'Etudes Structurales–CNRS, 29 rue J. Marvig, Boite Postale 4347, 31055 Toulouse Cedex, France.

*To whom correspondence should be addressed. E-mail: gim@zurich.ibm.com

ligand interactions; (ii) transition forces (100 to 300 pN) such as bond twists in dextran and of immunoglobulin (Ig)–like domains of titin; (iii) molecular spring constants, which range from 10 to 100 pN/nm and have persistence ranges from 0.4 nm for dextran (*10–13*). Comparison of experimental data with molecular dynamic simulations of force spectroscopy curves of single molecules (Fig. 2) illustrates the role of entropic forces in the flexibility of dextran filaments at low applied force, which is followed by changes in their molecular twist angle and finally by conformational changes at higher applied force, similar to recent observations in glucopyranose rings of polysaccharides (*11*, *12*). Titin, a protein of striated muscle, exhibits an entire series of discontinuous reversible unfoldings of individual Ig-like domains (*13*). SMFS studies have shown that molecular recognition and rupture processes are stochastic. Their mechanical properties trigger binding and unbinding and can be activated by random thermal motion. Beyond these fundamental insights, the mechanical properties of selectin and titin are directly related to their physiological function.

Tip Functionalization

To investigate single molecules, the physics and chemistry of a tip should be well defined and tailored for its specific application; a clear example of this is SMFS. The technology of fabricating atomically "perfect" and molecularly terminated apexes continues to improve and has a wide range of potential applications. The coating of tips with catalysts to induce reactions locally or with metals to deposit metallic clusters has been demonstrated (*14*). C_{60} molecules attached to STM tips and nanotubes are geometrically and structurally appealing probes for AFM imaging (*15*) because they combine molecular dimensions with extreme ruggedness. A new class of carbon nanostructures, graphitic cones (*16*), possesses unique characteristics that could also provide atomically perfect tips with excellent mechanical stability. Chemical functionalization of carbon nanotubes has recently been reported by coupling basic, hydrophobic, or biochemical terminations of the carboxyl groups to the open tip ends (*17*). These "smart" tubes represent an elegant step toward the ultimate single-molecular probe (*17*). Specific chemical binding of pairs of molecules, one sited on the tip, the other on the surface, such as biotin-avidin or conjugated DNA strands (*18*), is now being commercially developed in combination with magnetic bead technology used for immunoassays (*19*).

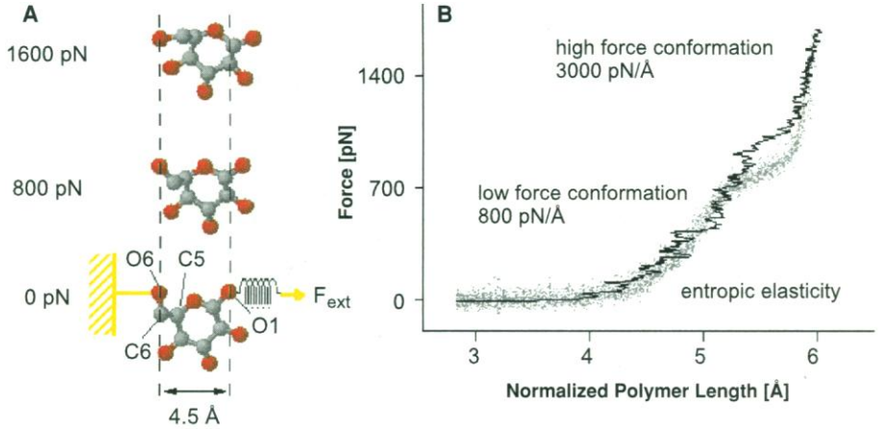

Fig. 2. Molecular dynamics calculations of the deformation of dextran using SMFS. (**A**) Ring conformations at different extension forces. (**B**) Normalized force versus extension force versus elongation of a five-glucose unit of dextran in water extended by entropic contributions (black curve). The gray dotted curve is a superposition of 10 normalized curves measured on native dextran. The spring constant was chosen as 70 mN/m. As in the AFM experiment, the exerted force was measured by Hooke's law by observing the deflection of the cantilever. The pulling velocity was chosen as 0.025 nm/ps. This figure is from (*12*).

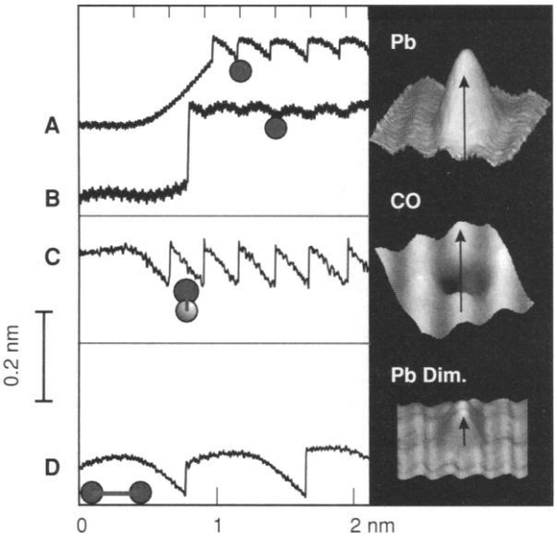

Fig. 3. Characteristic signatures for lateral repositioning of atomic and diatomic species. Left: Tip-height curves during manipulation on a Cu(211) surface along the [110] direction. (**A** and **B**) pulling and sliding a Pb atom; (**C**) pushing a CO molecule, in which the species move in registry with the underlying atomic lattice; and (**D**) a Pb dimer, which shows a lack of registry while being repositioned. The vertical marks correspond to face-centered cubic atomic sites. The sphere models indicate the initial sites of the manipulated species. The right panel shows STM images of the species; arrows indicate the direction of tip movement. This figure is adapted from (*23*).

Molecular Manipulation: Pushing, Pulling, Sliding

Manipulation of individual molecules can be used to build new molecular suprastructures, to explore the influence of the environment on a molecule, or to realize and test concepts for new nanodevices. Molecular manipulation in which the molecule remains intact without fragmentation is typically divided into vertical and lateral processes. Lateral processes usually govern the fundamental nanoengineering operation of repositioning molecules. Over the past few years, much has been learned from experiments and theoretical modeling of the underlying molecular nanomechanics. Tip-induced molecular motion was initially observed as a consequence of imaging at different tip proximities (*20*). In 1991, low-temperature atom and small-molecule manipulations were performed first on Xe and later on CO molecules (*21*). An example of a nanoexperiment based on atom repositioning is the "quantum corral," an electronic nanoresonator formed by a perfect circle of atoms with a diameter of 14.2 nm (*22*). Lateral translation of atoms, clusters, and molecules can be defined in terms of pulling, sliding, and pushing modes between the tip apex and the adsorbate. Each mode has a characteristic signature that is measurable from the feedback loop or the error signals of the STM during the translation process (or both) (Fig. 3). Pulling (Fig. 3A) and sliding (Fig. 3B) modes are based on weak attractive interactions in which the tip, respectively, precedes or remains on top of the atom or molecule and jumps from one substrate atom site to another (*23–25*). In contrast, Pb dimers (Fig. 3D) follow the tip in a discontinuous manner. Pushing, in which the molecule advances the tip and performs single hops along the substrate lattice, was observed with CO, which appears in Fig. 3C as a depression (*23*). Detailed analyses of manipulation dynamics promise to provide detailed information about diffusion barriers, the influence of defects, and

chemical reactivity.

The first demonstration of a two-dimensional (2D) translation of intact molecules at room temperature was achieved using a novel molecular architecture based on a rigid porphyrin core with four "legs" comprised of DTBP groups (*7*). The molecule-surface interaction is defined by weak, nondissociative Cu-methyl bonds. Six molecules were controllably translated across atomically clean Cu(100) surfaces into a hexagonal structure by lowering the tip toward the surface and translating it (Fig. 1, E and F). STM images of the molecule's characteristic four-lobed structure were particularly useful for assessing the orientation and integrity of the molecule before and after repositioning.

The translational characteristics of complex organic molecules differ from those of atoms or simple molecules and involve molecular flexure and reorientation of their conformation. Large molecules preferentially spend their interaction energy internally before overcoming a diffusion barrier. Modeling of the controlled translation of Cu-TDBPP at room temperature has shown that the dominant mode for molecular translation is pushing (*7*). Molecular mechanics simulations (Fig. 1G) indicate that lateral tip motion at close tip-surface distances results in tip-molecule contact followed by significant conformational changes, which build up and finally dissipate by a stick-slip translation motion of the molecule across the surface (Fig. 1H) (*7*). Room-temperature repositioning of molecules involves additional considerations, particularly molecular shape. One of the reasons for the success of controlled motion in Cu-TDBPP is that two of the four DTBP legs stabilize the tip-molecule interaction. Spherical molecules, on the other hand, are found to be less controllable because it is energetically favorable for such a molecule to avoid the tip by escaping sideways. This was observed in the repositioning of C_{60} deposited on a monolayer of bianthrone molecules and on Si(100) (*26*). Patterned templates can be used to stabilize and define molecular translation. The preferential adsorption of C_{60} at monatomic steps on Cu(111) results in a higher coordination of C_{60}, which in turn facilitates immobilization. Experiments were conducted on 10 C_{60} molecules adsorbed on such a step to demonstrate a molecular "abacus" that operated by the reversible and controllable translation of each of the 10 molecules along the step. Pushing required a threshold tip height defined by a tunnel resistance of ≈1 megohm, as compared to a tip-molecule contact resistance of C_{60} of 54 megohm (*27*).

The controlled translation of molecules on surfaces is thus governed by a delicate balance of the molecule-surface diffusion barrier and the interaction of the tip with the molecule. The latter is adjustable by tip proximity (and in STM by the applied voltage). Furthermore, in the pushing mode, the stabilization of the molecule's coordinates with respect to those of the tip and the internal mechanics of the molecule itself are also crucial. Design considerations for translatable molecules can be identified from current research. They include the separation of molecular functionality defining the tip-molecule interaction from the components involved in molecule-surface interaction. The molecule's conformational adaptability can be used to increase its lateral diffusion barrier by allowing multiple contacting atoms to find a minimum energy configuration (*28*). Conversely, tip-induced changes in molecular conformation can substantially lower the translation barrier.

Inelastic Tunneling in Single Molecules

Inelastic electron tunneling (IET) processes permit energy to be input into a single-molecular system to perform spectroscopic studies or as a means to selectively excite chemical bonds. IET spectroscopy was an important technique in the solid-state era of tunneling junctions (*29*). However, it took considerable time before the use of STM for molecular vibrational spectroscopy and other processes such as selective cleavage of chemical bonds was experimentally realized, despite its prediction in the mid-1980s (*30*). The first evidence of inelastic tunneling in STM was found in the resonant excitation of optically radiative, localized, electromagnetic modes between a metallic tip and sample (*31*). Light emission mediated by fullerene molecules was later demonstrated by this approach (*32*). Only in the past few years have dissociational, vibrational, rotational, and translational modes been investigated in depth. Vertical manipulation processes such as tip-surface hopping of single CO molecules were recently observed at energies sufficient to occupy their 2-π–derived antibonding states on Cu(111). Such hopping was measured to occur with a probability of 5×10^{-3} per tunneling electron (*33*). At large bias voltage, resonant IET processes have been invoked as being responsible for decomposing decaborane molecules and breaking the Si–H bond (*34*). Selective bond breaking on a hydrogenated Si(100) by STM has been used as the basis for ultra–high-resolution lithography (*35*). STM-based dissociation of O_2 molecules on Pt(111) occurs by exciting O–O stretch modes, and STM images have revealed details of the fragmentation process (*36*). Selective bond breaking has even been demonstrated for complex molecules containing ≈200 atoms (*37*). This suggests that weak bonds can be selectively tailored into molecular systems, permitting the synthesis of new molecular systems that are inaccessible by conventional chemistry.

A truly unique IET spectroscopic probe for single molecules (*38*) was demonstrated in the recent measurement of detailed vibrational spectra of individual acetylene molecules adsorbed on Cu(100), using a low-temperature STM with a reported vertical stability of 0.001 nm. Owing to the stringent requirements for observing the small inelastic component superimposed on the large elastic background of current-voltage spectra, it was necessary to accumulate the data over some 10 hours while tracking the molecule with the STM.

At low bias voltage, inelastic events can also be used to promote (enhance) the diffusion of a single adsorbate or an intramolecular activity (rotation or conformation change). STM has been used to induce rotation in single O_2 molecules at 8 K (Fig. 4) (*39*). The molecule was observed to rotate between three equivalent positions on Pt(111) surfaces. Rotation required activation by voltage pulses. The rotation rate

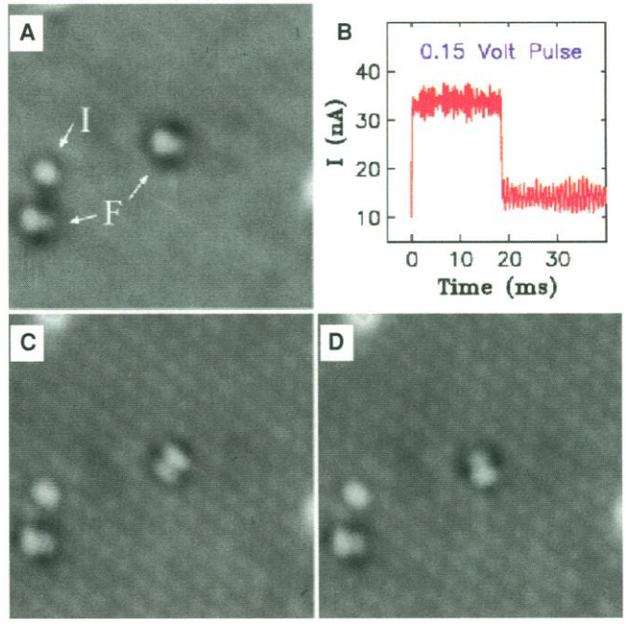

Fig. 4. Molecular rotation of an O_2 molecule on Pt(111) induced by tunneling. (**A**) STM image of two pear-shaped O_2 molecules on face-centered cubic, threefold hollow sites, with one next to a defect. I indicates a defect; F indicates O_2. (**B**) Current during a 0.15-V pulse over the isolated molecule in the center of the image, showing the moment of rotation (the step at ≈20 ms). (**C**) After-pulse image showing the second orientation of the molecule. (**D**) STM image taken after a second pulse, with the molecule rotated in the third orientation. This figure is from (*39*).

was found to vary with current (*39*). At low temperature, an intramolecular conversion of the tunneling vibronic energy into rotation on a C_2H_2 molecule adsorbed on Cu(100) has been reported (*40*). This observation implies that the inelastic tunneling energy is not completely redistributed at random within the vibronic manifold of the molecule. Some of it is redirected toward the rotational mode of C_2H_2 in its adsorption site before thermalization. It is not yet clear whether this partial selectivity of the intramolecular energy redistribution can be used in a large molecule to control the rotation of an intramolecular rotor or to activate a specific unimolecular reaction. Spatial mapping of the acetylene intramolecular vibration mode with the STM was also achieved (*38*), creating the opportunity to observe the spatial path of intramolecular energy redistribution processes in a single molecule.

Driving and observing a single chemical reaction are very attractive because the reaction barrier is lower on a catalytic surface (*41*). However, only a few attempts using STM to manipulate the reactants have been reported to date. Locally induced chemistry can also be conducted mechanically at zero applied voltage by reducing the surface dissociation barrier and letting thermal fluctuations at close tip proximity extract atoms, as demonstrated for Ge adatoms on Ge(111) (*42*). Going beyond local unimolecular reactions requires some form of molecular manipulation to drive two or more reactants toward the surface reaction pathway, as for the $CO + O \rightarrow CO_2$ reaction on Pt(111) (*43*).

A Molecular Rotor in a Supramolecular Bearing

STM-based molecular recognition, supramolecular interactions, and motional barriers below and above the thermal energy (kT), where k is Boltzmann's constant and T is the temperture (300 K), are the ingredients for the recent observation of a molecular rotor which was found to operate within a supramolecular bearing at room temperature (*44*). The molecule hexa-*tert*-butyl decacyclene is a propellor-shaped entity about 1.5 nm in diameter. High rigidity is imparted in its structure by steric interactions between the three blades of the decacyclene core, preventing the *tert*-butyl appendages from adapting to the underlying Cu(100) lattice. This provides the molecule with a very low diffusion barrier. At just below one full monolayer of coverage, most of the molecules are immobilized into a hexagonal 2D layer by steric crowding. In nanoscopic voids, individual molecules, which are normally resolved as six-lobed structures, were observed as a torus form of similar dimensions, pointing to single-molecular rotation. In certain voids, the molecules could be switched from a high-symmetry site with respect to the molecular lattice to low-symmetry sites (*44*) by a lateral molecular translation of one atomic spacing to the copper substrate (Fig. 5, A and B). These low-symmetry sites were shown to stabilize the lateral position of the molecule through supramolecular interactions while still providing a rotation barrier below the thermal energy at 300 K—which is sufficient to drive rotational motion. STM images of a single-molecule rotor in operation provide detailed molecular coordinates of the supramolecular bearing, which were used for molecular mechanical simulations (Fig. 5, C and D). The observation of the rotor raises interesting questions regarding the role of the second law of thermodynamics when applied to discrete nanoscale devices. Consider a particular case on the nanoscale in which useful work might be extracted from thermal noise: an individual nanodevice attached to a thermal reservoir. Here a colored (that is, partially correlated) noise from an independent source such as a tunnel current (*39*) must be applied to convert the thermal noise into useful work (*45*). In such a scheme, almost all the energy expended by the colored noise can be used to rectify thermal noise. Consequently, a nanodevice can, at least in theory, be designed to energetically approach the thermodynamic limit. The particular advantage of the nanoscale is that conventional limitations such as friction, wear, and inertia are bypassed. The application of nonequilibrium fluctuations in rectifying thermal noise without a thermal gradient has been discussed by Astumian (*45*). Nature itself uses such concepts in the rotary mechanics of ATP synthase, interpreted in terms of Brownian rotational fluctuations, which are converted into directed rotation by a chemical pawl action (*46*). The design of molecular machines that could harness noise usefully rather than being limited by it raises questions that may well be technologically decisive in the quest for highly dense nanoscale devices operating with near-perfect energy efficiency.

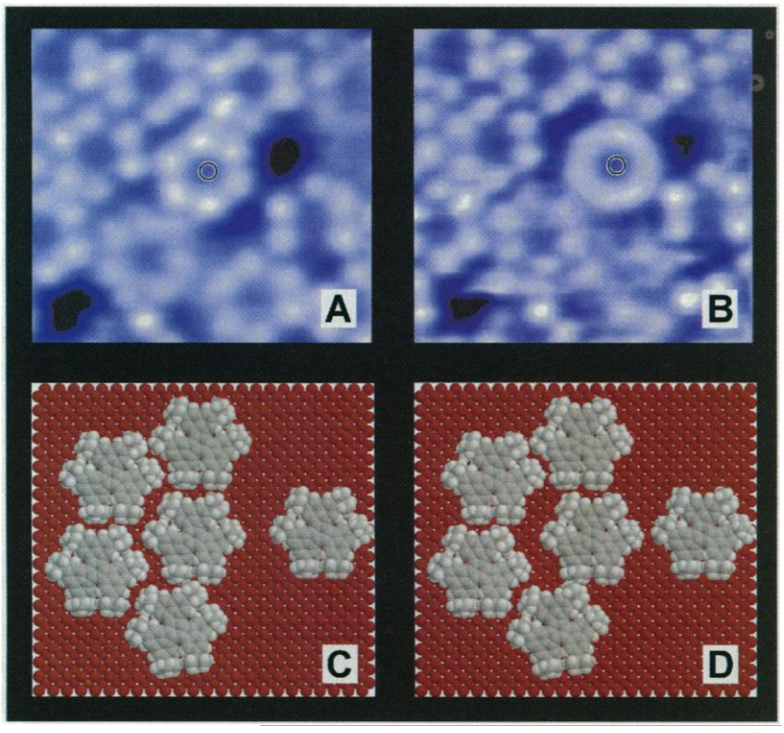

Fig. 5. Single-molecule rotor operating within a supramolecular bearing at room temperature. (**A** and **B**) STM images of hexa-*tert*-butyl decacyclene molecules at just below monolayer coverage on Cu(100). (A) In a nanoscopic void, the central molecule is imaged as a six-lobed structure (see circle) and is immobilized at a high-symmetry site defined by the surrounding molecules. In (B), a lateral translation by one Cu lattice spacing (0.26 nm) shifts the molecule to a lower symmetry site where it is imaged as a torus, indicating rotation (image area: 5.75 nm by 5.75 nm). (**C** and **D**) Snapshots of the molecular mechanical simulations based on the molecular coordinates taken from the STM data. The central rotor was rotated to compute the rotational barriers in the fixed and rotating states, which were found to be above and below room temperature, respectively. This figure is from (*44*).

Molecular Electronic Devices

Although molecular electronics have been the subject of much interest and speculation over the past 20 years, the electrical transport properties and working embodiments of single molecules have only recently become accessible to experiments. Single-walled nanotubes connected to nanoelectrodes can behave as coherent quantum wires, but recent STM images and tunneling spectroscopy have shown that they exhibit a large range of electronic characteristics, from metallic to semiconducting, which were found to depend on the tube diameter as well as their wrapping angle in terms of a

rolled-up graphene sheet (*47*). Field-effect transistors have been fabricated and tested using both single-walled and distorted multiwall tubes (*48*). Detailed investigations of mechanical distortions of bent tubes and tubes crossing tubes show that they can exhibit substantial tubular deformations as well as bending and buckling, a factor that has been suggested to influence their electrical device characteristics (*49*).

Molecular electronics devices have also been developed from measurements of the electrical resistance of a single C_{60} molecule defined by an electrical and mechanical contact that exhibits minimum mechanical deformation of the junction (*27*). Experimental and theoretical studies reveal that applying nanonewton-range forces to a single C_{60} molecule locally changes its electrical conductance continuously and reversibly. This effect was used to demonstrate a voltage amplifier employing a single molecule as the active element (*50*). The device is based on reversible conformational changes in the C_{60} cage structure by applying a force from a mechanical gate to the molecule. Tunneling through atoms and molecules whose filled and unfilled electronic states do not lie in the region around the Fermi level occurs by a process known as virtual (off-) resonance tunneling (*51*) at low applied voltages. Electrical resistance of the junction at contact is defined by the electronic transparency of the molecule. Transparency is a measure of the molecule's efficiency to extend the metallic wave function of the electrodes. The tails of the molecular orbitals, in particular those of the highest occupied and lowest unoccupied orbitals, provide such an extension (*52*) and are very sensitive to changes in hybridization and degeneracy induced by external distortion. For example, a distortion of 0.1 nm is sufficient to change the current flow through C_{60} by a factor of 100. Increasing this distortion leads to unity transparency, equivalent to a quantum unit of conductance $2e^2/h$, where e is the elementary charge and h is Planck's constant. Molecular extension of the metallic wave function is particularly relevant to devices operating at low voltages and where linear current-voltage characteristics are desirable. On the other hand, Coulomb blockade effects were observed for C_{60} molecules when they were deposited on an insulating layer at 4.2 K (*53*). Here wave-function decoupling of molecules is suggestive of a single-electron device using a molecule as an ideal quantum dot (*54*).

Perspective and Outlook

The nanomechanical properties of individual molecules take the form of vibrations, rotations, conformational changes, and translations. Inelastic tunneling processes, tip-induced forces, and Brownian motion have been found to drive mechanical responses in individual molecules. The important role of thermal noise at room temperature in nanoscale systems suggests that future technologies for building small energy-efficient devices will have to learn to use kT rather than fight against it. Future developments in single-molecule nanoscale science call for an even closer integration of chemistry, biology, physics, and technology in terms of synthesis, theoretical modeling, and advanced SPM techniques.

Although SPM has been shown to be an ultimate probe for investigating the properties of individual molecules, it is still an open question whether SPM has the intrinsic capabilities to be a useful fabrication tool in technology. The recent development of massive micromechanical arrays of thousands of SPM probes suggests that such a possibility is becoming more real each day. The further miniaturization of such probes would enable a suitable overlap of the scales of molecular mechanical systems and Si-based micromechanical tools. The increasing degree of both structural and molecular control of tips also supports such expectations. Mechanical properties related to scanning speed, density of devices, and stability all scale well with decreasing dimensions and may eventually provide advantages over electronics in terms of energy dissipation approaching the thermodynamic limit. However, major challenges exist in connecting multiple devices to the real world. Through design, synthesis, and experimentation, there is certainly much more room at the "bottom" to increase molecular complexity and functionality, which will expand our communication and promulgate exciting science on an individual molecular basis.

References and Notes

1. E. Schrödinger, *Br. J. Philos.* (1952), p. 233.
2. R. P. Feynman, *Sci. Eng.* **23**, 22 (1960).
3. G. Binnig, H. Rohrer, Ch. Gerber, E. Weibel, *Phys. Rev. Lett.* **49**, 57 (1982).
4. G. Binnig and H. Rohrer, *Rev. Mod. Phys.* **59**, 615 (1987); ———, in *Trends in Physics 1984*, J. Janta and J. Pantoflicek, Eds. (European Physical Society, The Hague, 1984), vol. 1, p. 38.
5. J. K. Gimzewski, E. P. Stoll, R. R. Schlittler, *Surf. Sci.* **181**, 267 (1987); D. P. E. Smith *et al.*, *Proc. Natl. Acad. Sci. U.S.A.* **84**, 969 (1987); D. P. E. Smith, M. D. Kirk, C. F. Quate, *J. Chem. Phys.* **86**, 6034 (1987).
6. H. Ohtani, R. J. Wilson, S. Chiang, C. M. Mate, *Phys. Rev. Lett.* **60**, 2398 (1988); P. Sautet and C. Joachim, *Chem. Phys. Lett.* **185**, 23 (1991).
7. T. A. Jung, R. R. Schlittler, J. K. Gimzewski, H. Tang, C. Joachim, *Science* **271**, 181 (1996).
8. M. T. Cuberes, R. R. Schlittler, T. A. Jung, K. Schaumburg, J. K. Gimzewski, *Surf. Sci.* **383**, 37 (1997); P. Moriatry, Y. R. Ma, M. D. Upward, P. H. Beton, *ibid.* **407**, 27 (1998).
9. F. Charra and J. Cousty, *Phys. Rev. Lett.* **80**, 1682 (1998).
10. J. Fritz, A. G. Katopodis, F. Kolbinger, D. Anselmetti, *Proc. Natl. Acad. Sci. U.S.A.* **95**, 12283 (1998).
11. P. E. Marszalek, A. F. Oberhauser, Y. P. Pangt, J. M. Fernandez, *Nature* **396**, 661 (1998); M. Rief, J. M. Fernandez, H. E. Gaub, *Phys. Rev. Lett.* **81**, 4764 (1998).
12. M. Rief, F. Oesterhelt, B. Heymann, H. E. Gaub, *Science* **275**, 1295 (1997).
13. M. Rief, M. Gautel, F. Oesterhelt, J. M. Fernandez, H. E. Gaub, *ibid.* **276**, 1109 (1997).
14. B. J. McIntyre, M. Salmeron, G. A. Somorjai, *ibid.* **265**, 1415 (1994); D. M. Kolb, R. Ullmann, T. Will, *ibid.* **275**, 1097 (1997).
15. K. F. Kelly, *ibid.* **273**, 1371 (1996); H. Dai, J. H. Hafner, A. G. Rinzler, D. T. Colbert, R. E. Smalley, *Nature* **384**, 147 (1996).
16. A. Krishan, *Nature* **388**, 451 (1997).
17. S. S. Wong, E. Joselevich, A. T. Woolley, C. L. Cheung, C. M. Lieber, *ibid.* **394**, 52 (1998).
18. E. L. Florin, V. T. Moy, H. E. Gaub, *Science* **264**, 45 (1994); G. U. Lee, D. A. Kidwell, R. J. Colton, *Langmuir* **10**, 354 (1994); G. U. Lee, L. A. Chrisey, R. J. Colton, *Science* **266**, 771 (1994).
19. D. R. Baselt, G. U. Lee, K. M. Hansen, L. A. Chrisey, R. L. Colton, *Proc. IEEE* **85**, 672 (1997).
20. J. K. Gimzewski, J. H. Coombs, R. Möller, R. R. Schlittler, in *Molecular Electronics*, A. Aviram, Ed. (United Engineering Trustees, New York, 1989), p. 87.
21. D. M. Eigler and E. K. Schweizer, *Nature* **344**, 524 (1990); Z. Zeppenfeld, C. P. Lutz, D. M. Eigler, *Ultramicroscopy* **42-44**, 128 (1992)
22. M. F. Crommie, C. P. Lutz, D. M. Eigler, *Science* **262**, 219 (1993).
23. L. Bartels, G. Meyer, K.-H. Rieder, *Phys. Rev. Lett.* **79**, 697 (1997).
24. X. Bouju, Ch. Girard, H. Tang, C. Joachim, L. Pizzagalli, *Phys. Rev. B* **55**, 16498 (1997).
25. J. A. Stroscio and D. M. Eigler, *Science* **254**, 1319 (1991).
26. M. T. Cuberes, R. R. Schlittler, J. K. Gimzewski, *Surf. Sci.* **371**, L231 (1997).
27. C. Joachim, J. K. Gimzewski, R. R. Schlittler, C. Chavy, *Phys. Rev. Lett.* **74**, 2102 (1995).
28. T. A. Jung, R. R. Schlittler, J. K. Gimzewski, *Nature* **386**, 696 (1997).
29. R. C. Jaklevic and J. Lambe, *Phys. Rev. Lett.* **17**, 1139 (1966); S. K. Khanna and J. Lambe, *Science* **220**, 1345 (1983).
30. B. N. J. Persson and A. Baratoff, *Phys. Rev. Lett.* **59**, 339 (1987); B. N. J. Persson and J. E. Demuth, *Solid State Commmun.* **57** 769 (1986).
31. J. K. Gimzewski, J. K. Sass, R. R. Schlittler, J. Schott, *Europhys. Lett.* **8**, 435 (1989).
32. R. Berndt *et al.*, *Science* **262**, 1425 (1993).
33. L. Bartels *et al.*, *Phys. Rev. Lett.* **80**, 2004 (1998).
34. G. Dujardin, R. W. Walkup, Ph. Avouris, *Science* **255**, 1232 (1992); T. C. Shen *et al.*, *ibid.* **268**, 1590 (1995).
35. S. Watanabe, Y. A. Ono, T. Hashizume, Y. Wada, *Phys. Rev. B* **54**, R17308 (1996).
36. B. C. Stipe *et al.*, *Phys. Rev. Lett.* **78**, 4410 (1997).
37. J. K. Gimzewski, T. A. Jung, M. T. Cuberes, R. R. Schlittler, *Surf. Sci.* **386**, 101 (1997).
38. B. C. Stipe, M. A. Rezaei, W. Ho, *Science* **280**, 1732 (1998).
39. ———, *ibid.* **279**, 1907 (1998).
40. ———, *Phys. Rev. Lett.* **81**, 1263 (1998).
41. T. Zambelli, J. V. Barth, J. Wintterlin, G. Ertl, *Nature* **390**, 495 (1997).
42. G. Dujardin *et al.*, *Phys. Rev. Lett.* **80**, 3085 (1998).
43. J. Wintterlin, S. Volkening, T. V. W. Janssens, T. Zambelli, G. Ertl, *Science* **278**, 1931 (1997).
44. J. K. Gimzewski *et al.*, *ibid.* **281**, 531 (1998).
45. R. D. Astumian, *ibid.* **276**, 917 (1997).
46. W. Junge, H. Lill S. Engelbrecht, *Trends Biochem. Sci.* **22**, 411 (1997).
47. J. W. G. Wildoer, L. C. Venema, A. G. Rinzler, R. E. Smalley, D. Dekker, *Nature* **391**, 59 (1998).
48. S. J. Tans, R. M. Verschueren, C. Dekker, *ibid.* **393**, 49 (1998); R. Martel, T. Schmidt, H. R. Shea, T. Hertel, Ph. Avouris, *Appl. Phys. Lett.* **73**, 2447 (1998).
49. T. Hertel, R. E. Walkup, Ph. Avouris, *Phys. Rev. B.* **58**, 13870 (1998); T. Hertel, R. Martel, Ph. Avouris, *J. Phys. Chem. B* **102**, 910 (1998); A. Rochefort, D. R. Salahub, Ph. Avouris, *Chem. Phys. Lett.* **297**, 45 (1998).
50. C. Joachim and J. K. Gimzewski, *Proc. IEEE* **86**, 184 (1998).
51. ———, *Europhys. Lett.* **30**, 409 (1995); A. Yazdani, D. M. Eigler, N. Lang, *Science* **272**, 1921 (1996).
52. M. Magoga and C. Joachim, *Phys. Rev. B* **56**, 4722 (1997).
53. D. Porath and O. Milo, *J. Appl. Phys.* **81**, 2241 (1997)
54. M. A. Reed, C. Zhou, C. J. Muller, T. P. Burgin, J. M. Tour, *Science* **278**, 252 (1997).

55. This work was partially supported by the European Commission Future Emerging Technologies (FET) Information Society Technology (IST) Program.